In Vivo Tests of Implantable Antennas in Rats: Antenna Size and Inter-Subject Considerations

Asimina Kiourti, *Student Member, IEEE*, Konstantinos Psathas, *Student Member, IEEE*, Pavlos Lelovas, Nikolaos Kostomitsopoulos, and Konstantina S. Nikita, *Senior Member, IEEE*

***Abstract*—We propose and implement an experimental protocol for *in vivo* testing of implantable antennas in rats, which aims to quantify dependence of the exhibited resonance performance upon antenna size and inter–subject and surgical procedure variability. Two implantable antennas with occupied volumes of 204 and 399 mm^3 are tested inside three different rats, each. Investigations are carried out in the Medical Implant Communications Service (MICS) band (402–405 MHz). Inter–subject and surgical procedure variations are found to quite affect the exhibited reflection coefficient frequency response, with reduction in antenna size further increasing sensitivity. Compared to simulations, maximum deviations in the center resonance frequency within the bandwidth and 10 dB–bandwidth equal –6.5% and +30.2% for the 204 mm^3 antenna, and –1.7% and –14.9% for the 399 mm^3 antenna. Antenna radiation and safety performance is finally assessed for glucose monitoring applications.**

***Index Terms*—Implantable antenna, *in vivo*, Medical Implant Communications Service (MICS) band.**

I. Introduction

IMPLANTABLE medical devices (IMDs) with wireless telemetry capabilities are recently attracting significant scientific interest for a number of diagnostic and therapeutic applications [1] [2]. A key and critical component of a wireless IMD is the implantable antenna, i.e., the antenna which is integrated into the IMD to allow its (bi–directional) telemetry with exterior monitoring/control equipment. Implantable antenna design is highly intriguing, with the major challenges including miniaturization, bandwidth enhancement, patient safety, and improved radiation performance [3]. Experimental investigations used to confirm the validity of numerical simulations are most commonly performed inside phantoms, which are relatively easy and practical to implement (e.g., [4], [5]). However, *in vivo* testing of implantable antennas is also crucial in order to verify their performance within realistic multi–tissue environments in which electrical properties depend upon frequency as well as age, size, sex, temperature of the subject, etc.

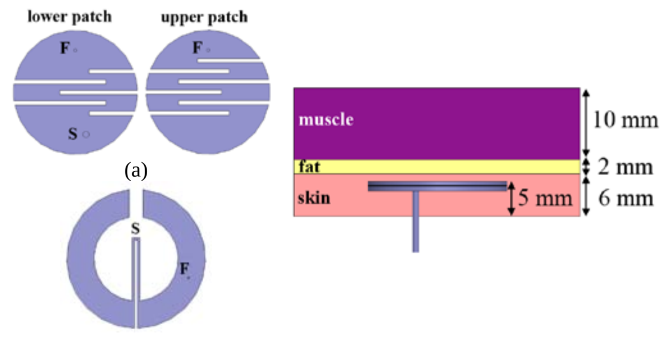

Fig. 1. Numerical simulations: (a) patch of the 204 mm^3 antenna, (b) patch of the 399 mm^3 antenna, and (c) simulation set–up.

In the literature, there exist only few recent studies on *in vivo* tests for implantable antennas. *In vivo* canine studies have been performed for an intracranial pressure implant with an integrated Planar Inverted F (PIFA) antenna operating in the Industrial, Scientific, and Medical (ISM) band (2.4–2.48 GHz) [6] [7]. The goal was to verify functionality of the device, and assess effectiveness of its packaging. Reflection coefficient measurements of a dual–band (Medical Implant Communications Service (MICS) (402–405 MHz) [8] and ISM bands) antenna implanted inside the dorsal midline of rats have also been presented [9]. A single experimental reflection coefficient frequency response was provided in the paper, which was denoted as the average among measurements carried out in three rats. Recently, *in vivo* testing of the aforementioned implantable antenna has further been carried out inside the caudal cervical area of two porcine subjects [10]. Two measured reflection coefficient frequency responses were provided, one for each subject. Temperature monitoring has, finally, been performed for an implantable sensor with an integrated multilayered spiral dual–band (MICS and ISM) antenna placed inside the back of a Göttingen minipig [11].

In this study, we propose an experimental protocol for *in vivo* testing of implantable antennas inside three different rats, and we implement it twice, i.e., considering two MICS implantable antennas with occupied volumes of 204 and 399 mm^3, respectively. The goal is to quantify dependence of the

Manuscript received June 06, 2013, revised August 11, 2013, accepted October 11, 2013. This work has been supported by the Operational Program "Education and Lifelong Learning" under the project ARISTEIA DEM-II-MED. The work of A. Kiourti was supported by the IEEE Microwave Theory and Techniques Society Graduate Fellowship for Medical Applications.

A. Kiourti, K.A. Psathas and K.S. Nikita are with the School of Electrical and Computer Engineering, National Technical University of Athens, Athens 15780, Greece (e-mail: akiourti@biosim.ntua.gr; kpsathas@biosim.ntua.gr, knikita@ece.ntua.gr).

P. Lelovas and N. Kostomitsopoulos are with the Center for Experimental Surgery, Biomedical Research Foundation Academy of Athens, Athens 11527, Greece (e-mail: paulveterin@yahoo.com; nkostom@bioacademy.gr) knikita@ece.ntua.gr).

exhibited reflection coefficient frequency response upon antenna size and inter–subject and surgical procedure variability. Surgeries and measurements are carried out in cooperation with and at the facilities of the Center for Experimental Surgery of the Biomedical Research Foundation Academy of Athens (CES–BRFAA). Measured and numerical results are provided, and quantitative inter–comparisons are given and discussed. Antenna radiation and safety performance is finally assessed for glucose monitoring applications.

II. Models and Methods

A. Implantable Antennas

Two implantable antennas of different sizes are considered for medical telemetry in the MICS band. Both antennas exhibit circular patch structures built on Rogers RO 3210 dielectric material (permittivity, ε_r = 10.2, loss tangent, tanδ = 0.003), are covered by a Rogers RO 3210 dielectric superstrate, include a shorting pin between the ground and patch planes (S), and are fed through a coaxial cable (F). The first antenna consists of two vertically–stacked meandered patches (Fig. 1(a)) and occupies a volume of 204 mm^3 (diameter of D = 12 mm). The second antenna includes a single ring–shaped patch (Fig. 1(b)) and occupies a volume of 399 mm^3 (D = 20 mm). Details regarding the design, prototype fabrication, and experimental testing of these antennas can be found in [12] and [13], respectively.

B. In Vivo Experimental Protocol

An experimental protocol is proposed for *in vivo* testing of implantable antennas, as shown in Fig. 2. The protocol addresses issues related to the: (a) type and number of model animals, (b) implantation site of the antenna, (c) anesthesia, (d) surgical procedure, (e) measurements, and (f) post–surgery treatment, and can be summarized as follows:

(a) Implantation and measurements are carried out inside rats, which have long been used in the literature as model animals [9]. Male Wistar outbred rats (HsdOla:WI) are employed, which are 16–17 weeks old, and exhibit a mean and standard deviation (SD) body weight of 331.3 ± 9.2 gr. In order to assess inter–subject and surgical procedure variability, each antenna is implanted and measured inside three different rats (serial numbers of i = 1–3).

(b) Since the antennas under study have been designed for operation inside soft–tissues, implantation is carried out within the subcutaneous tissue of the rats' abdomen.

(c) Each rat is first anesthetized with an intraperitoneal (i.p.) injection of 70 mg/kg ketamine (Ketaset, Fort Dodge, Iowa, USA) and 5mg/kg xylazine (Rompun, Bayer, Leverkusen, Germany).

(d) A wound with a length of (D + 5 mm) is further made in the rat's abdomen area, and the antenna is implanted within the abdominal subcutaneous tissue. Following implantation, the wound is closed with 0/4 silk sutures (Silkam, Braun, Aesculap, Tuttlingen, Germany), leaving a 2 mm opening for the feeding coaxial cable to exit the skin.

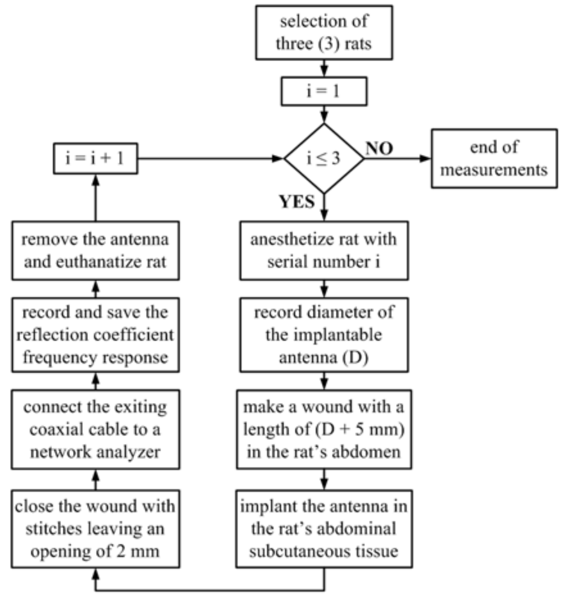

Fig. 2. Proposed *in vivo* experimental protocol for implantable antenna measurements in rats.

(e) Right after surgery, the feeding coaxial cable is connected to an Agilent Fieldfox handheld network analyzer (Agilent Technologies, Santa Clara, California, USA). The reflection coefficient frequency response exhibited by the antenna under study is further recorded and saved. Measurement is carried out within the 300 MHz to 500 MHz frequency range, which symmetrically covers the MICS band.

(f) Once measurement is completed, the implanted antenna is removed, and the rat is euthanized in a CO_2 chamber. Time lapse from the start of the surgical procedure to euthanasia of each rat does not exceed 8 min.

In vivo experimentation is conducted in compliance with the legal requirements regarding the care and use of laboratory animals in Greece.

III. Results

A. In Vivo Measurements

The *in vivo* experimental protocol of Fig. 2 is implemented twice, i.e., for the 204 and the 399 mm^3 implantable antennas of Fig. 1, respectively. Implantation and measurements are carried out in six rats, i.e., three different rats for each of the antennas under study. The implantable antenna prototypes and the experimental set–up used in this study are shown in Fig. 3. X–ray fluoroscopy images are provided in Fig. 4 to illustrate the exact implantation site for the antennas.

Measured reflection coefficient frequency responses are shown in Fig. 5(a) and Fig. 5(b) for the 204 mm^3 and the 399 mm^3 implantable antennas, respectively. Measurements within the three different rats are denoted in the legends as "rat 1", "rat 2", and "rat 3", respectively.

B. Analysis of Results and Discussion

For comparison purposes, numerical reflection coefficient frequency responses are super–imposed in Fig. 5 for each of

This is the author's version of an article that has been published in this journal. Changes were made to this version by the publisher prior to publication.
The final version of record is available at http://dx.doi.org/10.1109/LAWP.2013.2286818

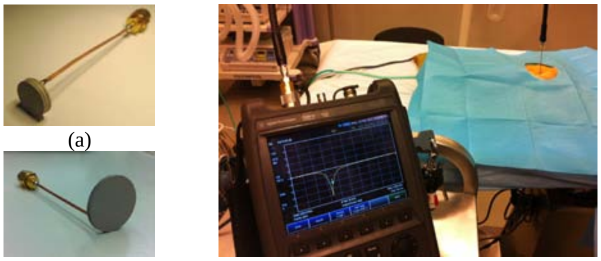

(a) (b) (c)

Fig. 3. In vivo measurements: (a) prototype of the 204 mm^3 antenna, (b) prototype of the 399 mm^3 antenna, and (c) experimental set–up.

(a) (b)

Fig. 4. X–ray fluoroscopy images indicating the antenna implantation site inside the rats: (a) face, and (b) profile views.

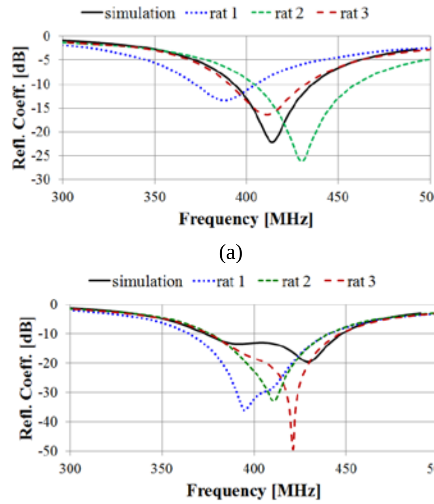

(a)

(b)

Fig. 5. Numerical and in vivo measured reflection coefficient frequency responses of the: (a) 204 mm^3, and (b) 399 mm^3 implantable antennas.

the antennas under study ("simulation"). Finite Element simulations have been performed in Ansoft HFSS considering the antennas to be placed 5 mm under the outer surface of a three–layer tissue model which simulates skin (ε_r = 46.7, σ = 0.69 S/m), fat (ε_r = 5.58, σ = 0.04 S/m), and muscle (ε_r = 57.1, σ = 0.79 S/m) properties at 402 MHz (Fig. 1(c)) [14]. Fig. 6(a) records the percentage change of the center resonance frequency measured within the bandwidth ($f_{res,m}$) as compared to the corresponding numerical value ($f_{res,n}$), i.e.,

$$\%\text{ change in } f_{res} = \frac{f_{res,m} - f_{res,n}}{f_{res,n}} \cdot 100 \quad (1)$$

The percentage changes in the exhibited 10 dB–bandwidths (BW) are calculated similarly, and are shown in Fig. 6(b).

As indicated in Fig. 4 and Fig. 5, numerical and experimental results exhibit quite good agreement. Compared to numerical simulations, percentage changes in f_{res} and BW are found to equal –6.5% and +30.2% for the 204 mm^3 antenna, and –1.7% and –14.9% for the 399 mm^3 antenna. Maximum deviations in f_{res} and BW recorded among the three measurements in different rats are found to equal 43 MHz and 23 MHz for the 204 mm^3 antenna, respectively, and 8 MHz, and 12 MHz for the 399 mm^3 antenna, respectively.

Deviations between experimental and numerical results, as well as between experimental results among different rats for the same antenna may be attributed to a number of factors which affect implantable antenna performance in *in vivo* experimentation. These can be summarized as follows: (a) air gaps between the implanted antenna and the surrounding tissues, (b) presence of multiple types of tissues around the antenna, (c) dependence of tissue electrical properties upon frequency, (d) inter–rat variability (anatomy and dependence of tissue electric properties upon each rat's age, size, internal body temperature etc), and (e) variations in the surgical procedures followed (implantation depth, implantation site, length of the wound, closure of the wound with sutures, etc).

Compared to the 204 mm^3 antenna, the 399 mm^3 antenna is found to exhibit smaller deviations in f_{res} and BW between experimental and numerical investigations, as well as between measurements in different rats. Results can be attributed to its, relatively, increased dimensions, which offer a considerably better control of the surgical implantation procedure. The increased surface area of the 399 mm^3 antenna offers enhanced stability of its placement within the tissues, while allowing for the antenna itself to be able to support the weight of the attached coaxial cable which exits the rats' skin. It is worth noting that in the case of the 204 mm^3 antenna, exterior support is required in order to hold the coaxial cable in a straight position and prevent it from dropping, and, thus, deteriorating antenna placement within the biological tissues.

Results indicate the significance of *in vivo* experimentation for implantable antennas in order to verify their functionality within realistic biological tissue environments, which occur to considerably differ from the respective numerical ones. Furthermore, the need for implantable antennas with wide impedance bandwidth is highlighted. The goal is to compensate for detuning and impedance mismatch issues inherent in inter–subject and surgical procedure variations. Finally, increase in implantable antenna size is shown to reduce sensitivity of the exhibited reflection coefficient frequency response to the aforementioned considerations. Setting wide impedance bandwidth and reduced sensitivity to detuning as goals for the performance of an implantable antenna, demonstrates the need for advanced antenna designs which do not solely emphasize on miniaturization.

IV. Antenna Radiation and Safety Performance

Radiation and safety performance of the implantable antennas under study is hereafter investigated for glucose monitoring applications. Implantation is performed inside the skin of an ellipsoidal trunk model, which consists of skin (thickness of 5 mm), fat (thickness of 10 mm), and muscle tissues (Fig. 7(a)). Origin of the coordinate system coincides

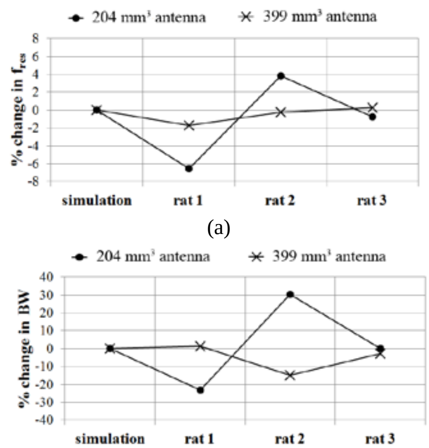

(b)

Fig. 6. Percentage changes of the following measured parameters, as compared to the corresponding numerical values: (a) center resonance frequency within the bandwidth (f_{res}), and (b) 10 dB–bandwidth (BW).

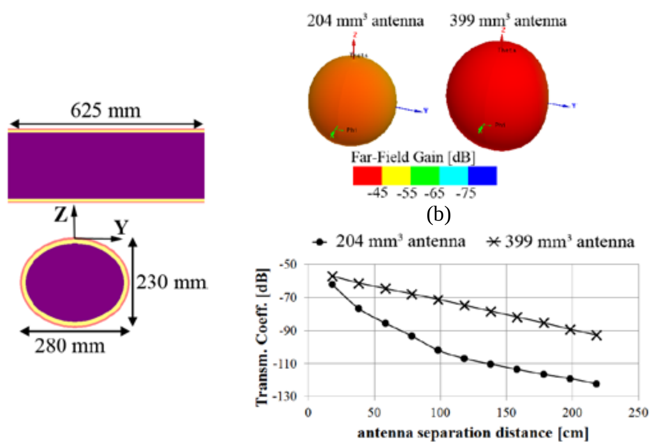

(a) (c)

Fig. 7. Antenna performance evaluation for glucose monitoring: (a) ellipsoidal trunk model, (b) far-field gain radiation patterns, and (c) transmission coefficient considering an exterior monopole antenna.

with the center of the antennas' ground plane. The 204 and 399 mm^3 antennas radiate nearly omni–directional far–field gain radiation patterns (Fig. 7(b)) with maximum gain values of –47.6 dB and –41.1 dB, respectively. Conformance with the IEEE C95.1–1999 patient safety restrictions is found to limit the maximum allowable net–input power to the antennas to 1.977 mW and 3.714 mW, respectively [15]. These power levels increase to 21.43 mW and 21.50 mW for conformance with the recent IEEE C95.1–2005 restrictions [15]. Fig. 7(c) records the transmission coefficient between an exterior MICS monopole antenna (ground plane on Z axis, monopole along the –Y axis) and each of the implantable antennas, as a function of distance. Assuming an exterior receiver sensitivity of –75 dBm and a transmitting power of 1.977 mW (2.96 dBm), the maximum telemetry range is limited to 40 cm and 138 cm for the 204 mm^3 and 399 mm^3 antennas, respectively.

V. Conclusion

In this study, reflection coefficient measurements were performed for two implantable antennas (volumes of 204 mm^3 and 399 mm^3), operating within the abdominal subcutaneous tissue of three different rats, each. The *in vivo* experimentation protocol was developed and implemented in cooperation with CES–BRFAA. Effects of live tissue as well as inter–subject and surgical procedure variability were shown to quite affect the exhibited reflection coefficient frequency response, with reduction in antenna size further increasing sensitivity. Compared to simulations, maximum deviations in f_{res} and BW were found to equal –6.5% and +30.2% for the 204 mm^3 antenna, and –1.7% and –14.9% for the 399 mm^3 antenna. Radiation and safety performance of the antennas under study was also investigated for glucose monitoring applications. Future investigations will include biococompatible encapsulation of the antennas and assessment of their performance for long–term *in vivo* operation.

References

[1] A. Kiourti, K.A. Psathas, and K.S. Nikita, "Implantable and ingestible medical devices with wireless telemetry functionalities," *Wiley Bioelectrom.* (to appear)

[2] A. Sani, A. Alomainy, and Y. Hao, "Numerical characterization and link budget evaluation of wireless implants considering different digital human phantoms," IEEE Trans. Microw. Theory Techn., vol. 58, pp. 2605 – 2613, Oct. 2009.

[3] A. Kiourti, and K.S. Nikita, "A review of implantable patch antennas for biomedical telemetry: challenges and solutions," *IEEE Antennas Propag. Mag.*, vol. 54, pp. 210–228, Jun. 2012.

[4] Z. Duan, Y.X. Guo, R.F. Xue, M. Je, and D.L. Kwong, "Differentially fed dual – band implantable antenna for biomedical applications," *IEEE Trans. Antennas Propag.*, vol. 60, pp. 5587–5595, Dec. 2012.

[5] C. J. Sánchez-Fernández, O. Quevedo–Teruel, J. Requena–Carrión, L. Inclán–Sánchez, and E. Rajo–Iglesias, "Dual-band microstrip patch antenna based on short-circuited ring and spiral resonators for implantable medical devices," *IET Microw. Antennas Propag.*, vol. 4, pp. 1048-1055, Aug. 2010.

[6] "International Telecommunications Union-Radiocommunications (ITU–R), Radio Regulations, Section 5.138 and 5.150," ITU, Geneva, Switzerland; available online: http://itu.int/home.

[7] U. Kawoos, M.–R. Tofighi, R. Warty, F.A. Kralick, and A. Rosen, "In–vitro and in–vivo trans–scalp evaluation of an intracranial pressure implant at 2.4 GHz," *IEEE Trans. Microw. Theory Techn.*, vol. 56, pp. 2356–2365, Oct. 2008.

[8] "Medical Implant Communications Service (MICS) Federal Register," *Rules Reg.*, vol. 64, pp. 69926-69934, Dec. 1999,.

[9] T. Karacolak, R. Cooper, J. Butler, S. Fisher, and E. Topsakal, "In vivo verification of implantable antennas using rats as model animals," *IEEE Antennas Wireless Propag. Lett.*, vol. 9, pp. 334–337, 2010.

[10] T. Karacolak, R. Cooper, E.S. Unlu, and E. Topsakal, "Dielectric properties of porcine skin tissue and in vivo testing of implantable antennas using pigs as model animals," *IEEE Antennas Wireless Propag. Lett.*, vol. 11, pp. 1686–1689, 2012.

[11] F. Merli, L. Bolomey, F. Gorostidi, B. Fuchs, J.F. Zurcher, Y. Barrandon, E. Meurville, J.R. Mosig, and A.K. Skrivervik, "Example of data telemetry for biomedical applications: an in vivo experiment," *IEEE Antennas Wireless Propag. Lett.*, vol. 11, pp. 1650–1654, 2012.

[12] A. Kiourti and K.S. Nikita, "Miniature scalp–implantable antennas for telemetry in the MICS and ISM bands: design, safety considerations, and link budget analysis," *IEEE Trans. Antennas Propag.*, vol. 60, pp. 3568 – 3575, Aug. 2012.

[13] A. Kiourti, J.R. Costa, C.A. Fernandes, and K.S. Nikita, "A broadband implantable and a dual–band on–body repeater antenna: design and transmission performance," *IEEE Trans. Antennas Propag.* (under review)

[14] C. Gabriel, S. Gabriel, and E. Corthout, "The dielectric properties of biological tissues," *Phys. Med. Biol.*, vol. 41, pp. 2231–2293, 1996.

[15] IEEE Standard for Safety Levels With Respect to Human Exposure to Radiofrequency Electromagnetic Fields, 3 kHz to 300 GHz, IEEE Standard C95.1, 1999, 2005.